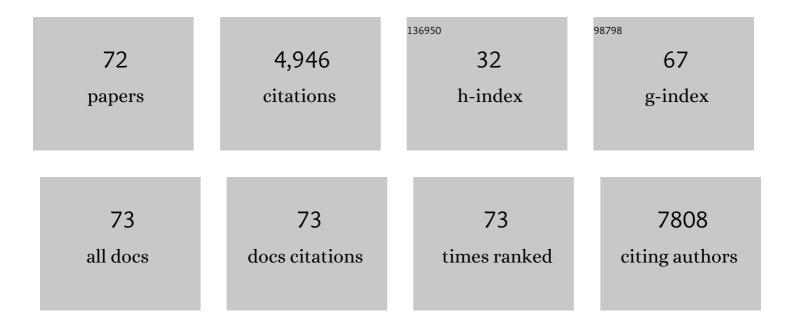
## David Bonekamp

List of Publications by Year in descending order

Source: https://exaly.com/author-pdf/4698950/publications.pdf Version: 2024-02-01



#	Article	IF	CITATIONS
1	Three-dimensional Magnetic Resonance Imaging–based Printed Models of Prostate Anatomy and Targeted Biopsy-proven Index Tumor to Facilitate Patient-tailored Radical Prostatectomy—A Feasibility Study. European Urology Oncology, 2022, 5, 357-361.	5.4	7
2	Repeatability and Reproducibility of ADC Measurements and MRI Signal Intensity Measurements of Bone Marrow in Monoclonal Plasma Cell Disorders. Investigative Radiology, 2022, 57, 272-281.	6.2	22
3	Impact of Surgeon's Experience in Rigid Versus Elastic MRI/TRUS-Fusion Biopsy to Detect Significant Prostate Cancer Using Targeted and Systematic Cores. Cancers, 2022, 14, 886.	3.7	3
4	Quantitative Analysis of DCE and DSC-MRI: From Kinetic Modeling to Deep Learning. RoFo Fortschritte Auf Dem Gebiet Der Rontgenstrahlen Und Der Bildgebenden Verfahren, 2022, , .	1.3	0
5	Pseudoprospective Paraclinical Interaction of Radiology Residents With a Deep Learning System for Prostate Cancer Detection. Investigative Radiology, 2022, Publish Ahead of Print, .	6.2	6
6	Detection of Significant Prostate Cancer Using Target Saturation in Transperineal Magnetic Resonance Imaging/Transrectal Ultrasonography–fusion Biopsy. European Urology Focus, 2021, 7, 1300-1307.	3.1	44
7	Standardized Magnetic Resonance Imaging Reporting Using the Prostate Cancer Radiological Estimation of Change in Sequential Evaluation Criteria and Magnetic Resonance Imaging/Transrectal Ultrasound Fusion with Transperineal Saturation Biopsy to Select Men on Active Surveillance. European Urology Focus. 2021. 7. 102-110.	3.1	28
8	Simulated clinical deployment of fully automatic deep learning for clinical prostate MRI assessment. European Radiology, 2021, 31, 302-313.	4.5	24
9	Comparison of Prostate MRI Lesion Segmentation Agreement Between Multiple Radiologists and a Fully Automatic Deep Learning System. RoFo Fortschritte Auf Dem Gebiet Der Rontgenstrahlen Und Der Bildgebenden Verfahren, 2021, 193, 559-573.	1.3	18
10	Magnetic resonance imagingâ€guided transurethral ultrasound ablation in patients with localised prostate cancer: 3â€year outcomes of a prospective Phase I study. BJU International, 2021, 127, 544-552.	2.5	13
11	The Value of Prostate-specific Antigen Density for Prostate Imaging-Reporting and Data System 3 Lesions on Multiparametric Magnetic Resonance Imaging: A Strategy to Avoid Unnecessary Prostate Biopsies. European Urology Focus, 2021, 7, 325-331.	3.1	34
12	Magnetic Resonance Imaging-Guided Transurethral Ultrasound Ablation of Prostate Cancer. Journal of Urology, 2021, 205, 769-779.	0.4	45
13	Reply by Authors. Journal of Urology, 2021, 205, 779-779.	0.4	1
14	Comparison of single-scanner single-protocol quantitative ADC measurements to ADC ratios to detect clinically significant prostate cancer. European Journal of Radiology, 2021, 136, 109538.	2.6	7
15	Fully Automatic Deep Learning in Bi-institutional Prostate Magnetic Resonance Imaging. Investigative Radiology, 2021, 56, 799-808.	6.2	27
16	Improvement of PI-RADS-dependent prostate cancer classification by quantitative image assessment using radiomics or mean ADC. Magnetic Resonance Imaging, 2021, 82, 9-17.	1.8	19
17	Measured Multipoint Ultra-High b-Value Diffusion MRI in the Assessment of MRI-Detected Prostate Lesions. Investigative Radiology, 2021, 56, 94-102.	6.2	9
18	Imaging of prostate cancer. Deutsches Ärzteblatt International, 2021, , .	0.9	8

#	Article	IF	CITATIONS
19	Single-Center Evaluation of Treatment Success Using Two Different Protocols for MRI–Guided Transurethral Ultrasound Ablation of Localized Prostate Cancer. Frontiers in Oncology, 2021, 11, 782546.	2.8	0
20	Combined Clinical Parameters and Multiparametric Magnetic Resonance Imaging for the Prediction of Extraprostatic Disease—A Risk Model for Patient-tailored Risk Stratification When Planning Radical Prostatectomy. European Urology Focus, 2020, 6, 1205-1212.	3.1	39
21	Automated volumetric assessment with artificial neural networks might enable a more accurate assessment of disease burden in patients with multiple sclerosis. European Radiology, 2020, 30, 2356-2364.	4.5	16
22	Twelve-month prostate volume reduction after MRI-guided transurethral ultrasound ablation of the prostate. European Radiology, 2019, 29, 299-308.	4.5	27
23	Automated brain extraction of multisequence MRI using artificial neural networks. Human Brain Mapping, 2019, 40, 4952-4964.	3.6	284
24	Classification of Cancer at Prostate MRI: Deep Learning versus Clinical PI-RADS Assessment. Radiology, 2019, 293, 607-617.	7.3	214
25	Prediction of significant prostate cancer in biopsy-naÃ <sup>-</sup> ve men: Validation of a novel risk model combining MRI and clinical parameters and comparison to an ERSPC risk calculator and PI-RADS. PLoS ONE, 2019, 14, e0221350.	2.5	13
26	Defective homologous recombination DNA repair as therapeutic target in advanced chordoma. Nature Communications, 2019, 10, 1635.	12.8	64
27	Automated quantitative tumour response assessment of MRI in neuro-oncology with artificial neural networks: a multicentre, retrospective study. Lancet Oncology, The, 2019, 20, 728-740.	10.7	271
28	Histopathological to multiparametric MRI spatial mapping of extended systematic sextant and MR/TRUS-fusion-targeted biopsy of the prostate. European Radiology, 2019, 29, 1820-1830.	4.5	24
29	Radiomics Based on Adapted Diffusion Kurtosis Imaging Helps to Clarify Most Mammographic Findings Suspicious for Cancer. Radiology, 2018, 287, 761-770.	7.3	81
30	Transcriptome Wide Analysis of Magnetic Resonance Imaging-targeted Biopsy and Matching Surgical Specimens from High-risk Prostate Cancer Patients Treated with Radical Prostatectomy: The Target Must Be Hit. European Urology Focus, 2018, 4, 540-546.	3.1	18
31	Radiomic subtyping improves disease stratification beyond key molecular, clinical, and standard imaging characteristics in patients with glioblastoma. Neuro-Oncology, 2018, 20, 848-857.	1.2	170
32	Multiparametric MRI fusion-guided biopsy for the diagnosis of prostate cancer. Current Opinion in Urology, 2018, 28, 172-177.	1.8	13
33	Multicentre evaluation of magnetic resonance imaging supported transperineal prostate biopsy in biopsyâ€naÃ⁻ve men with suspicion of prostate cancer. BJU International, 2018, 122, 40-49.	2.5	108
34	Simultaneous whole-body 18F–PSMA-1007-PET/MRI with integrated high-resolution multiparametric imaging of the prostatic fossa for comprehensive oncological staging of patients with prostate cancer: a pilot study. European Journal of Nuclear Medicine and Molecular Imaging, 2018, 45, 340-347.	6.4	32
35	Correlation between genomic index lesions and mpMRI and 68Ga-PSMA-PET/CT imaging features in primary prostate cancer. Scientific Reports, 2018, 8, 16708.	3.3	27
36	Multiparametric MRI and MRI/TRUS Fusion Guided Biopsy for the Diagnosis of Prostate Cancer. Advances in Experimental Medicine and Biology, 2018, 1096, 87-98.	1.6	3

DAVID BONEKAMP

#	Article	IF	CITATIONS
37	<i>NRG1</i> Fusions in <i>KRAS</i> Wild-Type Pancreatic Cancer. Cancer Discovery, 2018, 8, 1087-1095.	9.4	189
38	Radiomic Machine Learning for Characterization of Prostate Lesions with MRI: Comparison to ADC Values. Radiology, 2018, 289, 128-137.	7.3	162
39	Voxel-wise radiogenomic mapping of tumor location with key molecular alterations in patients with glioma. Neuro-Oncology, 2018, 20, 1517-1524.	1.2	36
40	Diffusionâ€weighted MRI treatment monitoring of primary hypofractionated proton and carbon ion prostate cancer irradiation using raster scan technique. Journal of Magnetic Resonance Imaging, 2017, 46, 850-860.	3.4	8
41	Prediction of malignancy by a radiomic signature from contrast agentâ€free diffusion MRI in suspicious breast lesions found on screening mammography Journal of Magnetic Resonance Imaging, 2017, 46, 604-616.	3.4	113
42	Improved detection of melanoma metastases by iodine maps from dual energy CT. European Journal of Radiology, 2017, 90, 27-33.	2.6	14
43	Combined Clinical Parameters and Multiparametric Magnetic Resonance Imaging for Advanced Risk Modeling of Prostate Cancer—Patient-tailored Risk Stratification Can Reduce Unnecessary Biopsies. European Urology, 2017, 72, 888-896.	1.9	136
44	T1ï•weighted Dynamic Glucose-enhanced MR Imaging in the Human Brain. Radiology, 2017, 285, 914-922.	7.3	72
45	The Value of PSA Density in Combination with PI-RADSâ,,¢ for the Accuracy of Prostate Cancer Prediction. Journal of Urology, 2017, 198, 575-582.	0.4	179
46	Local recurrence of prostate cancer after radical prostatectomy is at risk to be missed in 68Ga-PSMA-11-PET of PET/CT and PET/MRI: comparison with mpMRI integrated in simultaneous PET/MRI. European Journal of Nuclear Medicine and Molecular Imaging, 2017, 44, 776-787.	6.4	124
47	Potential of quantitative susceptibility mapping for detection of prostatic calcifications. Journal of Magnetic Resonance Imaging, 2017, 45, spcone.	3.4	2
48	Adiabatically prepared spinâ€lock approach for T1ïâ€based dynamic glucose enhanced MRI at ultrahigh fields. Magnetic Resonance in Medicine, 2017, 78, 215-225.	3.0	71
49	Potential of quantitative susceptibility mapping for detection of prostatic calcifications. Journal of Magnetic Resonance Imaging, 2017, 45, 889-898.	3.4	54
50	Multicentre evaluation of targeted and systematic biopsies using magnetic resonance and ultrasound imageâ€fusion guided transperineal prostate biopsy in patients with a previous negative biopsy. BJU International, 2017, 120, 631-638.	2.5	104
51	Mask-Adapted Background Field Removal for Artifact Reduction in Quantitative Susceptibility Mapping of the Prostate. Tomography, 2017, 3, 96-100.	1.8	9
52	Early Detection of Malignant Transformation in Resected WHO II Low-Grade Glioma Using Diffusion Tensor-Derived Quantitative Measures. PLoS ONE, 2016, 11, e0164679.	2.5	8
53	Radiogenomics of Glioblastoma: Machine Learning–based Classification of Molecular Characteristics by Using Multiparametric and Multiregional MR Imaging Features. Radiology, 2016, 281, 907-918.	7.3	236
54	Integration of genomics and histology revises diagnosis and enables effective therapy of refractory cancer of unknown primary with <i>PDL1</i> amplification. Journal of Physical Education and Sports Management, 2016, 2, a001180.	1.2	57

DAVID BONEKAMP

#	Article	IF	CITATIONS
55	Radiomic Profiling of Glioblastoma: Identifying an Imaging Predictor of Patient Survival with Improved Performance over Established Clinical and Radiologic Risk Models. Radiology, 2016, 280, 880-889.	7.3	345
56	Dynamic contrast enhanced MRI monitoring of primary proton and carbon ion irradiation of prostate cancer using a novel hypofractionated raster scan technique. Radiotherapy and Oncology, 2016, 120, 313-319.	0.6	10
57	Clinical parameters outweigh diffusion- and perfusion-derived MRI parameters in predicting survival in newly diagnosed glioblastoma. Neuro-Oncology, 2016, 18, 1673-1679.	1.2	36
58	Multiparametric Magnetic Resonance Imaging (MRI) and MRI–Transrectal Ultrasound Fusion Biopsy for Index Tumor Detection: Correlation with Radical Prostatectomy Specimen. European Urology, 2016, 70, 846-853.	1.9	258
59	MR Perfusion–derived Hemodynamic Parametric Response Mapping of Bevacizumab Efficacy in Recurrent Glioblastoma. Radiology, 2016, 279, 542-552.	7.3	51
60	Susceptibilityâ€based analysis of dynamic gadolinium bolus perfusion MRI. Magnetic Resonance in Medicine, 2015, 73, 544-554.	3.0	19
61	Association of overall survival in patients with newly diagnosed glioblastoma with contrast-enhanced perfusion MRI: Comparison of intraindividually matched T <sub>1</sub> - and T <sub>2</sub> <sup>*</sup> -based bolus techniques. Journal of Magnetic Resonance Imaging, 2015, 42, 87-96.	3.4	61
62	High-dose methotrexate with or without rituximab in newly diagnosed primary CNS lymphoma. Neurology, 2014, 83, 235-239.	1.1	120
63	Interobserver agreement of semi-automated and manual measurements of functional MRI metrics of treatment response in hepatocellular carcinoma. European Journal of Radiology, 2014, 83, 487-496.	2.6	63
64	Castleman Disease: The Great Mimic. Radiographics, 2011, 31, 1793-1807.	3.3	180
65	Advancements in MR Imaging of the Prostate: From Diagnosis to Interventions. Radiographics, 2011, 31, 677-703.	3.3	215
66	Quantitative SENSE-MRSI of the human brain. Magnetic Resonance Imaging, 2010, 28, 305-313.	1.8	30
67	Diffusion tensor imaging in children and adolescents: Reproducibility, hemispheric, and age-related differences. NeuroImage, 2007, 34, 733-742.	4.2	247
68	Fast method for brain image segmentation: Application to proton magnetic resonance spectroscopic imaging. Magnetic Resonance in Medicine, 2005, 54, 1268-1272.	3.0	12
69	Maki effect. , 0, , 168-170.		Ο
70	Gibbs ringing artifact. , 0, , 154-158.		0
71	Inappropriate inversion time selection for late gadolinium enhancement imaging. , 0, , 146-149.		0
72	Pseudostenosis on time-of-flight magnetic resonance angiography. , 0, , 165-167.		0